Barbaros Çetin[1,2]
Dongqing Li[3]

[1]Mechanical Engineering, Middle East Technical University, Northern Cyprus Campus, Güzelyurt, Turkey
[2]Mechanical Engineering Department, Bilkent University, Ankara, Turkey
[3]Department of Mechanical and Mechatronics Engineering, University of Waterloo, Waterloo, Ontario, Canada

Received March 15, 2011
Revised June 9, 2011
Accepted June 9, 2011

Review

Dielectrophoresis in microfluidics technology

Dielectrophoresis (DEP) is the movement of a particle in a non-uniform electric field due to the interaction of the particle's dipole and spatial gradient of the electric field. DEP is a subtle solution to manipulate particles and cells at microscale due to its favorable scaling for the reduced size of the system. DEP has been utilized for many applications in microfluidic systems. In this review, a detailed analysis of the modeling of DEP-based manipulation of the particles is provided, and the recent applications regarding the particle manipulation in microfluidic systems (mainly the published works between 2007 and 2010) are presented.

Keywords:
Dielectrophoresis / Lab-on-a-chip / Microfluidics / Particle manipulation
DOI 10.1002/elps.201100167

1 Introduction

Lab-on-a-chip (LOC) devices are microfluidic platforms that can handle complex chemical and biological management and analysis for many practical applications in the fields of life sciences, space explorations, defense industry, atmospheric sciences, pharmaceutical research, etc. The manipulation of particles in LOC systems is crucial in a variety of diagnostic and clinical applications such as trapping, sorting, separation and patterning, characterization, purification of cells, viruses, nanoparticles, microparticles and proteins [1–99]. To manipulate particles, various techniques have been developed to be used in microsystems such as optical tweezers [1], magnetophoresis [2], acoustic means [3] and electrical means. Electrical forces such as electrophoresis (EP) and dielectrophoresis (DEP) are the subtle solution to manipulate particles in LOC devices due to their favorable scaling for the reduced size of the system [100]. EP is the movement of the electrically charged particles in an electrical field due to the Columbic body force acting on the particles because of their surface charge. EP is commonly used in conventional and well-developed separation techniques such as capillary electrophoresis to separate DNA, proteins, etc. DEP is the movement of particles in a non-uniform electric field due to the interaction of the particle's dipole and spatial gradient of the electric field. Among other methods, DEP is one of the most popular methods for particle manipulation in microsystems due to (i) its label-free nature, (ii) its favorable scaling effects [100], (iii) the simplicity of the instrumentation and (iv) its ability to induce both negative and positive forces. DEP force depends on the size and the electrical properties of the particles and the suspending medium. DEP is applicable even for non-conducting particles and can be generated either by using direct current (DC) or alternating current (AC) field. DC-DEP [4–16], AC-DEP [17–90] and DC-biased AC-DEP [91–99] have been successfully implemented for the manipulation of micro/nanoparticles.

Common practice for DC-DEP applications is that the electric field is applied by using external electrodes that are submerged into the reservoirs, and the flow is also induced by the electric field (i.e. EOF). The non-uniform electric field is generated by means of the specially designed structures inside the microchannel network such as electrically insulated hurdles and obstacles, and it is called insulator-based DEP (iDEP). There is no electrode inside the device; therefore, these devices are robust, chemically inert and very simple in terms of fabrication. Since external electrodes are used, DC-DEP needs high voltage to generate sufficient DEP force which may lead to a serious Joule heating effect inside the channel. This severe temperature increase inside the channel due to Joule heating may lead to a bubble formation which can severely disturb the operation of the device [101]. Furthermore, even slightly increasing the temperature ($\Delta T \approx 4^{\circ}C$ above physiological cell temperature) inside the channel may lead to cell death for in vivo mammalian cell experiments [100].

Correspondence: Dr. Barbaros Çetin, Mechanical Engineering Department, Bilkent University, 06800 Ankara, Turkey
E-mail: barbaros.cetin@bilkent.edu.tr, barbaroscetin@gmail.com
Fax: +90-312-290-4126

Abbreviation: AC-DEP, alternating current dielectrophoresis; **CM,** Clausius–Mossotti factor; **CNT,** carbon nanotube **DC-DEP,** direct current dielectrophoresis; **DEP,** dielectrophoresis/dielectrophoretic; **EP,** electrophoresis/electrophoretic; **iDEP,** insulator-based dielectrophoresis; **LOC,** lab-on-a-chip; **MST,** Maxwell-stress tensor; **n-DEP,** negative dielectrophoresis; **p-DEP,** positive dielectrophoresis; **ROT,** electrorotation; **twDEP,** traveling-wave DEP

Colour Online: See the article online to view Fig. 8 in colour.

Common practice for AC-DEP applications is that an array of metal electrodes (i.e. interior electrodes) is embedded inside the microchannel network. Most of the time, these internal electrodes are planar (2-D) ones (i.e. height of the electrodes are in the order of hundred nanometers), and are fabricated within the device by means of complex, time-consuming and relatively expensive manufacturing techniques such as chemical vapor deposition and e-beam evaporation, which results in less economically feasible systems as the system scale increases. Moreover, while working with bioparticles, fouling of the electrodes may distort the operation of the device [10]. In spite of its drawbacks, AC-DEP is advantageous due to the low operating voltage that prevents Joule heating. Moreover, low voltages simplify the equipment needed to generate the electric fields, makes AC-DEP the system compatible with integrated circuits and suitable for battery powered hand-held devices.

In this review, a detailed insight of the DEP phenomenon for DC-DEP and AC-DEP applications is provided and the modeling of DEP-based manipulation of the particles for DC-DEP and AC-DEP systems is presented. Recent applications regarding the particle manipulation in microfluidic systems are presented. Future research directions for dielectrophoretic manipulation of the particles are also addressed.

2 Dielectrophoresis

DEP is the movement of a particle in a non-uniform electric field due to the interaction of the particle's dipole and spatial gradient of the electric field. The particle's dipole has mainly two origins. The first is the permanent dipole which is due to the orientation of the atoms, and it inherently exists. The second is the induced dipole which is due to the reorientation of the charges on the particle's surface with the presence of the external electric field. To discuss the induced dipole in detail, the concept of polarizability needs to be introduced. Polarizability can be described as the measure of the ability of a material to produce charge at the interface (interfacial polarization (more generally, polarizability is the measure of the ability of the material to respond to an electric field, which has three basic mechanisms, namely (i) electronic polarization, (ii) atomic polarization and (iii) orientational polarization. Interfacial polarization is the additional mechanism that is due to the accumulation of charges at the interface of two different dielectrics. Our discussion of polarizability is limited with interfacial polarizability since it is the origin of the induced dipole on particles for the operating frequencies of 10 kHz to 100 MHz [102, 103]. When a particle is suspended in an electrolyte and placed in an electric field, the charges inside the particle and inside the medium will be redistributed at the particle–medium interface depending on the polarizability of the particle and the medium. If the polarizability of the particle is higher than that of the medium, more charges will accumulate at the particle's side. If the polarizability of the medium is higher than that of the particle, more charges will accumulate at the medium's side. This non-uniform distribution of the charges means a difference in the charge density on either side of the particle which leads to an induced dipole across the particle aligned with the applied electric field. When the particle–medium system is placed in a non-uniform electric field, the particle feels different forces at each end (see Fig. 1 for the case of a spherical particle). The difference in force at both ends generates a net force in either direction depending on the polarizability of the particle and the medium.

There are two methods to calculate the DEP force on a particle, (i) point-dipole method and (ii) Maxwell-stress tensor (MST) formulation.

(i) Point-dipole method

The essence of this method is that the particle is replaced by an equivalent point-charge dipole that would generate the same electrical potential distribution around the particle. The force on a dipole in an electric field can be written as [102, 104]

$$\mathbf{F} = (\mathbf{p} \cdot \nabla)\mathbf{E} \tag{1}$$

where bold letters refer to a vector quantity, $\mathbf{p}$ is the dipole moment, $\mathbf{E}$ is the electric field. In this expression, the induced higher order multipolar moments other than dipole moment are neglected. The neglection of these higher order multipolar moments is acceptable for moderate non-linear electric fields [105] which is the typical case for DEP-based LOC devices. For the extreme cases where the particle is located in a strong field gradient or near a field null, the induced higher order multipolar moments should be taken into account, and the force equation should be modified accordingly. Force equations where the induced higher order multipolar moments are taken into account have been derived and can be found elsewhere [106, 107].

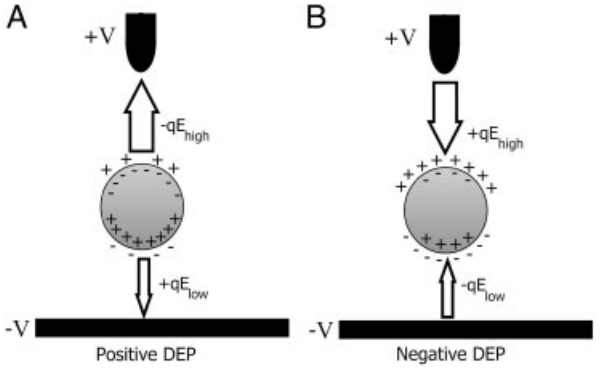

Figure 1. DEP force on an induced dipole with the presence of a non-uniform electric field. (A) Positive-DEP; (B) Negative-DEP.

(ii) MST formulation

In this method, the stress induced at the particle surface due to the electrical potential distribution needs to be determined, and the stress tensor, which is called MST, $\underline{\mathbf{T}}$, needs to be integrated over the surface of the particle as follows [107]:

$$\mathbf{F}_{\mathrm{DEP}} = \oint_S (\underline{\mathbf{T}} \cdot \mathbf{n})\, \mathrm{d}S \tag{2}$$

where $\mathbf{n}$ is unit vector normal to the surface and $\underline{\mathbf{T}}$ is defined as

$$\underline{\mathbf{T}} = \varepsilon(\mathbf{E} \otimes \mathbf{E} - \frac{1}{2}\mathbf{E}^2\underline{\mathbf{U}}) + \mu(\mathbf{H} \otimes \mathbf{H} - \frac{1}{2}\mathbf{H}^2\underline{\mathbf{U}}) \tag{3}$$

where $\mathbf{E}$ and $\mathbf{H}$ are the electric and magnetic fields, respectively, $\underline{\mathbf{U}}$ is the unit tensor and symbol $\otimes$ denotes the dyadic product. For an applied electric field with a frequency less than 100 MHz, effects due to the magnetic field components (i.e. second bracket in the stress tensor equation) can be ignored, which is known as near-field approximation [107].

The DEP force on a spherical particle can be derived by using either of these methods. Both methods give identical expressions for this special case. The detailed derivation of the dielectrophoretic force on a spherical particle by using point-dipole method [106, 108] and by using MST formulation [107] can be found elsewhere. During the derivation of the DEP force in both approaches, there is a critical step where the field at the surface of the particle is required to be expanded in terms of the original field at the particle center. The limitation of this critical step is that it has a slightly non-uniform field and it is valid if the particle size is small compared with the spatial variation of the electric field (i.e. the size of the particle is much smaller than the distance over which the external electric field varies) [109]. For a more accurate calculation of the DEP force in case of a high non-uniformity, the induced higher order dipole moments [106, 107] need be introduced into the point-dipole approach. On the other hand, for the MST formulation, the electrical field distribution can be determined on the particle surface by means of a numerical method, and the stress distribution on the particle can be determined by using Eq. (3). Then DEP force can be calculated by integrating $\underline{\mathbf{T}} \cdot \mathbf{n}$ over the particle surface as shown in Eq. (2).

The dielectrophoretic force on a spherical particle can be formulated as

$$\mathbf{F}_{\mathrm{DEP}} = 2\pi\varepsilon_{\mathrm{m}} f_{\mathrm{CM}} R^3 \nabla(\mathbf{E} \cdot \mathbf{E}) = 2\pi\varepsilon_{\mathrm{m}} f_{\mathrm{CM}} R^3 \nabla|\mathbf{E}|^2 \tag{4}$$

where $\mathbf{E}$ is the electric field, ε_{m} is the absolute permittivity of the suspending medium and R is the particle radius. f_{CM} is the Clausius–Mossotti (CM) factor, which is given by

$$f_{\mathrm{CM}} = \frac{\varepsilon_{\mathrm{p}} - \varepsilon_{\mathrm{m}}}{\varepsilon_{\mathrm{p}} + 2\varepsilon_{\mathrm{m}}} \tag{5}$$

where ε is the permittivity, and subscripts "p" and "m" stand for the particle and the medium, respectively. Note that when $\varepsilon_{\mathrm{p}} > \varepsilon_{\mathrm{m}}$, f_{CM} becomes positive, and when $\varepsilon_{\mathrm{p}} < \varepsilon_{\mathrm{m}}$, f_{CM} becomes negative. If the limit $\varepsilon_{\mathrm{m}} \to \infty$ is taken, f_{CM} becomes $-1/2$; and if the limit $\varepsilon_{\mathrm{p}} \to \infty$ is taken, f_{CM} becomes 1. It can be concluded that CM factor has numerical limits as -0.5 and 1.0.

As mentioned before, Eq. (4) can be modified to take the higher order multipolar moments into account. The dielectrophoretic force on a spherical particle including dipole and quadrupole moments can be formulated as [108]

$$\mathbf{F}_{\mathrm{DEP}} = 2\pi\varepsilon_{\mathrm{m}} f_{\mathrm{CM}} R^3 \nabla|\mathbf{E}|^2 + \frac{2}{3}\pi\varepsilon_{\mathrm{m}} f_{\mathrm{CM}} R^5 \nabla \cdot \nabla|\mathbf{E}|^2 \tag{6}$$

Close examination of Eq. (4) may help us to understand the favorable scaling of DEP phenomena. Suppose that L denotes the length that characterizes the electrical field variations and ϕ denotes the applied voltage to the system. For a fixed size of particle, an order of magnitude estimate of DEP force using Eq. (4) would lead to

$$\mathbf{F}_{\mathrm{DEP}} \sim \frac{\phi^2}{L^3} \tag{7}$$

This means scaling down a system with $L \sim 1$ cm to a system with $L \sim 100\,\mu$m (which is the typical size for LOC devices) same DEP force can be obtained with a $\sim$1000 times reduced voltage. Thus, with low voltages, sufficient DEP force can be generated. Low voltage means simple instrumentation and simple circuitry which is crucial for a robust and/or a hand-held device. By using the same approach, temperature rise of the system as a result of the Joule heating ($\propto \sigma\mathbf{E}^2$) can be written as [100]

$$\Delta T \sim L^2|\mathbf{E}|^2 \tag{8}$$

which means for a given electric field strength, the temperature rise would reduce by the reduction of the system size.

In order to manipulate particles and cells by utilizing DEP, the magnitude of the DEP force should be large enough to dominate other forces such as drag force, electrothermal forces, buoyancy force, AC electro-osmotic force and the Brownian motion. Drag force is the result of the interaction of the particle with the flow field. Electrothermal forces result from the electrical body force due to the permittivity and conductivity gradients within the fluid due to the temperature gradients as a result of Joule heating or as a result of external heating such as illumination from the optical detection system. Moreover, the temperature gradient within the fluid can also generate buoyancy force. AC-electro-osmotic force is the result of interaction of the particle with the fluid flow induced on the surface of the coplanar electrodes when an AC-field is applied. Brownian motion is the random movement of particles due to the thermal effects. Although DEP force is tunable by means of other parameters like molarity of the suspending medium and the electrical field, the tunable range of these parameters is restricted due to some constraints (e.g. usage of high electric fields may lead to Joule heating, temperature rise and the electrolysis of the suspending medium; usage of the high-conductivity buffer solutions may cause undesired electrothermal effects and excessive osmotic stress in the case of biological analytes) [110]. Therefore, the order of

magnitude estimate of the various forces experienced by a particle is crucial for DEP-based applications to predict the resultant motion of the particles. Typically, electrothermal forces dominate at high frequency (high frequency indicates frequency much larger that charge relaxation frequency, $\omega\varepsilon/\sigma$) and high voltages, AC electro-osmotic force dominates at low frequency, and Brownian motion is negligible for the particles with a size larger than 1 μm for microfluidic applications [111]. Detailed analysis of the scaling of various forces with system parameters can be found elsewhere [110, 111].

For the DEP application with internal electrodes, the interfacial effects may occur at the interface between the fluid medium and the electrode surface, and may lead to electrode polarization due to the discontinuity of the charge carrier species between the metal and the liquid suspension (current is carried by electrons in metal and by ions in suspensions). Electrode polarization leads to an electric potential loss in the suspension (i.e. lower applied voltage and lower DEP force felt by the particle) and to a reduction in the particle manipulation capabilities. It may also lead to local heating around the electrodes which may result in AC electroconvection [105], bubble formation and dissolution of the electrodes [100] any of which may affect the performance of the device or disrupt the operation of the device. Therefore, electrode polarization needs to be avoided. For the suspensions with conductivities higher than 100 mS/m and/or systems operating at frequencies higher than 10 kHz, electrode polarization is typically avoided [105].

2.1 Dielectropheric force in an AC-Field

In the case of an AC-field with a single frequency ω, the time-dependent variables in the system can be represented by using phasor notation. The electric field can be represented as

$$\mathbf{E}(\mathbf{x},t) = \mathrm{Re}[\hat{\mathbf{E}}(\mathbf{x})\mathrm{e}^{\mathrm{j}\omega t}] \tag{9}$$

where $\hat{\mathbf{E}} = (-\nabla\hat{\phi})$ is the electric field phasor (**E** thereafter). In the case of an AC-field, the permittivities in the f_{CM} term must be replaced by complex permittivities. Performing this substitution leads to a complex dipole moment expression as [104]

$$\tilde{\mathbf{p}} = 4\pi\varepsilon_m f_{CM} R^3 \mathbf{E} \tag{10}$$

where

$$f_{CM}(\tilde{\varepsilon}_p, \tilde{\varepsilon}_m) = \frac{\tilde{\varepsilon}_p - \tilde{\varepsilon}_m}{\tilde{\varepsilon}_p + 2\tilde{\varepsilon}_m} \tag{11}$$

where $\tilde{\varepsilon}$ is the complex permittivity and defined as

$$\tilde{\varepsilon} = \varepsilon - \mathrm{j}\left(\frac{\sigma}{\omega}\right) \tag{12}$$

By using the phasor notation, time-averaged DEP force on a spherical particle in an AC-field can be expressed as [112]

$$\langle \mathbf{F}_{DEP}(t) \rangle = 2\pi\varepsilon_m \mathrm{Re}[f_{CM}] R^3 \nabla \mathbf{E}_{rms}^2 \tag{13}$$

where E_{rms} is the root-mean-square magnitude of the applied AC electric field and f_{CM} is the CM factor and is defined in Eq. (11).

Some important features of the DEP phenomena can be listed as follows by the close examination of Eq. (13):

(i) DEP is a non-linear phenomena due to dependence on the electrical field strength ($\mathbf{E}^2$ term).
(ii) DEP force is present only when the electric field is non-uniform.
(iii) DEP force does not depend on the polarity of the electric field.
(iv) DEP force is proportional to particle volume (DEP has the potential to manipulate particles by their sizes).
(v) DEP force is proportional to electrical properties of the particle and the medium (the permittivities and the conductivities of the particle and the medium), and the frequency of the field (DEP has the potential to manipulate particles by their electrical properties).
(vi) DEP force depends on the sign and the magnitude of the CM factor, f_{CM}. If $f_{CM} > 0$, then the particles will be attracted by the electric field strength maxima and repelled from minima (*p-DEP*). If $f_{CM} < 0$, then the particles will be attracted by the electric field strength minima and repelled from maxima (*n-DEP*).

By combining Eqs. (12) and (11), CM factor can be written in the form as

$$f_{CM}(\varepsilon_p, \sigma_p, \varepsilon_m, \sigma_m, \omega) = \frac{(\varepsilon_p - \varepsilon_m) + \mathrm{j}/\omega(\sigma_p - \sigma_m)}{(\varepsilon_p + 2\varepsilon_m) + \mathrm{j}/\omega(\sigma_p + 2\sigma_m)} \tag{14}$$

By the close examination of Eq. (14), it can be deduced that the sign of the CM factor is determined by the electrical conductivities of the particle and the medium at low frequencies; however, it is determined by the permittivities at higher frequencies. The frequency response of these two typical cases is given in Fig. 2 for some given input parameters. In both cases, the curves have two asymptotic limits referring the two extremes, namely low- and high-frequency response. Between those limits there exits a transition region. In both figures, the case where the electrical conductivity of the particle is equal to that of the medium has the zero $\mathrm{Re}[f_{CM}]$. During the transition, the DEP response switches between n-DEP and p-DEP. The point where n-DEP response switches to the p-DEP (or p-DEP response switches to n-DEP) is called cross-over frequency. It is the point where the complex permittivity of the particle is exactly equal to the that of the medium. At that frequency, DEP force will be zero (i.e. $\mathrm{Re}[f_{CM}] = 0$). As seen in Fig. 2A, for case (i), the cross-over frequencies are almost the same for all curves (except those where the conductivity of the particle is equal to that of the medium). As seen in Fig. 2B, for case (ii), the cross-over frequency is shifting to the right as the conductivity of the medium increases. Case (i) is a typical response characteristic of the system formed by polystyrene (latex) particles (solid, homogeneous, spherical particles) suspending in an aqueous medium. In Fig. 2, the electrical conductivity of the

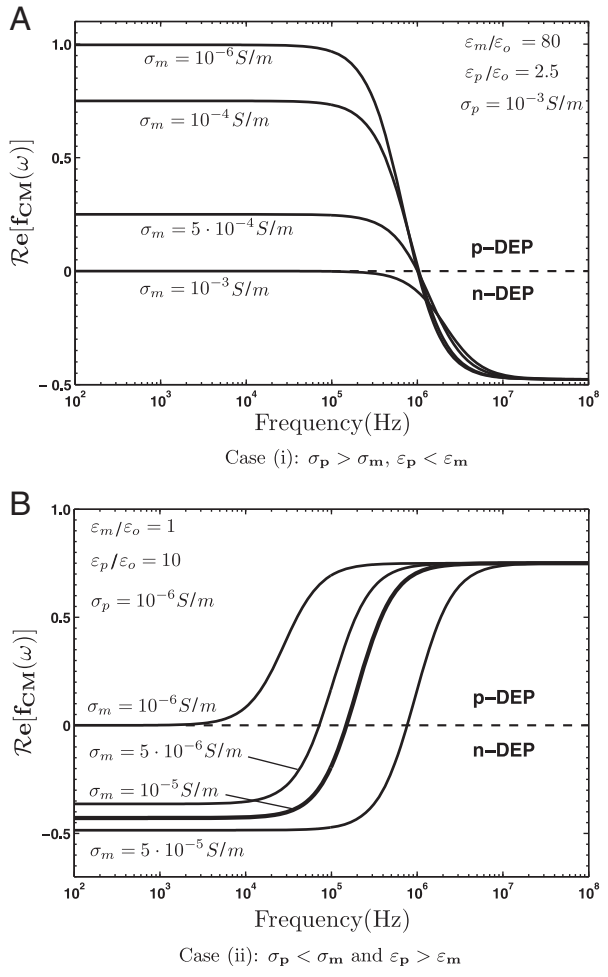

Figure 2. DEP spectra of a dielectric sphere. (A) Case (i): $\sigma_p > \sigma_m$, $\varepsilon_p < \varepsilon_m$. (B) Case (ii): $\sigma_p < \sigma_m$ and $\varepsilon_p > \varepsilon_m$.

particle are held constant and the DEP response for different medium conductivities are plotted.

Although a particle's complex permittivity is defined in a simple expression in terms of its bulk permittivity and the bulk electrical conductivity, it is usually more complicated than that due to some interfacial phenomena occurring at the particle–medium interface. The interface between the particle and medium introduces an additional shell, which has its own distinct dielectric properties. The importance and the complexity of this interfacial phenomena increases as the particles size decreases (the detailed physical picture of the interfacial phenomena can be found elsewhere [108]). Therefore, DEP response of a micron- or larger-sized particles may differ from that of the nano-sized particles or molecules [105]. Although polymer-based materials have low bulk conductivity ($\sigma_{bulk} \cong 0$), micron-sized or nano-sized polymer-based particles may have high particle conductivity due to the interfacial phenomena. The conductivity of sphere particles can be expressed by using the concept of surface conductance as [113]

$$\sigma_p = \sigma_{bulk} + \frac{2\lambda}{R} \tag{15}$$

where R is the particle radius and λ is the surface conductance (typically ln S for latex particles) [114, 115]. Therefore, the electrical conductivity of the micro/nanoscale particles depend upon the size of the particles.

Time-averaged DEP force, Eq. (13), is valid for a stationary AC-field. If the phase of the AC-field has a spatial variation, Eq. (13) needs to be modified to include this effect. In general sense, time-averaged DEP force can be written as

$$\langle \mathbf{F}_{DEP}(t) \rangle = 2\pi\varepsilon_m \mathrm{Re}[f_{CM}] R^3 \nabla \mathbf{E}^2_{rms} + 4\pi\varepsilon_m \, \mathrm{Im}[f_{CM}] R^3 \times (\mathbf{E}^2_{rms,i} \nabla \varphi_i) \tag{16}$$

where φ is the phase of the AC-field. Subscript i refers to each component of the electric field and the phase gradient. The last term in the parenthesis is a tensor notation and refers to the summation of the components of the vector quantities inside the bracket. Im[·] refers to the imaginary part of a complex quantity. The first term depends on the non-uniformity in the electric field strength, and second term depends on the non-uniformity in the phase of the electric field which is the driving force for the traveling-wave DEP (twDEP) applications. In the case of series of planar electrodes patterned at the bottom substrate of an LOC device which are excited with different phases, the first term leads to a levitation for particles with n-DEP response, and the second term leads to an axial motion of the particles over the electrodes, see Fig. 3. Direction of the axial motion depends on the sign of the imaginary part of the CM.

2.2 Dielectropheric force in a DC-Field

When DC-field (or AC-field with low frequency) is applied, the DEP force expressions remain the same; however, CM factor depends solely on electrical conductivities of the medium and the particle and is expressed as [4–9, 98]

$$f_{CM}(\sigma_p, \sigma_m) = \frac{(\sigma_p - \sigma_m)}{(\sigma_p + 2\sigma_m)} \tag{17}$$

For the case of living cells, the main contribution for the CM comes from the membrane of the cell. In DC field, electric field drops across the cell membrane and living cells behave like poorly conductive particles (i.e. $\sigma_p \cong 0$), which results in a negative CM [4, 5]. Therefore, the DEP motion of cells under the DC field can be well modeled by n-DEP [6, 8], and the DEP force in a DC-field for a living cell with a

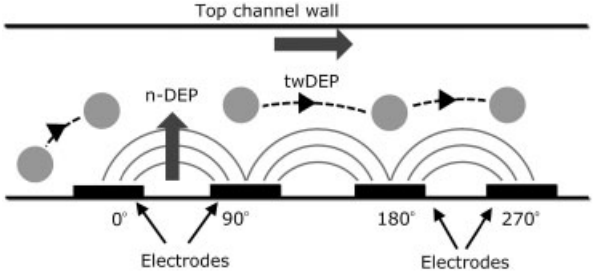

Figure 3. Schematic illustration of twDEP motion of a particle.

low-cell membrane conductivity can be written as [6–9]

$$\mathbf{F}_{\mathrm{DEP}} = -\pi\varepsilon_{\mathrm{m}} R^3 \nabla \mathbf{E}^2 \tag{18}$$

2.3 Dielectrophoretic force on biological particles

DEP has also been implemented for the manipulation of biological particles such as bacteria, viruses, spores, yeast and other eukaryotic cell types as well as proteins, nucleic acids and other biomolecules [116]. These biological particles have a more complicated internal structure than that of a solid, homogeneous particle. Although these complications do not change fundamental physics, the expressions accounting for the dipole moment and the DEP force needs to be modified to take into account these complications. The common approach to theoretically model the biological particles is to use a concentric multi-shell model [102]. The simplest case is the single, spherical shell model [104, 117]. In this model, a homogeneous sphere with an effective complex permittivity of $\tilde{\varepsilon}'_{\mathrm{p}}$ is substituted with the original two-layered particle (Fig. 4). An effective homogeneous complex permittivity value, $\tilde{\varepsilon}'_{\mathrm{p}}$, replaces the $\tilde{\varepsilon}_{\mathrm{p}}$ in the CM factor as

$$f_{\mathrm{CM}}(\tilde{\varepsilon}'_p, \tilde{\varepsilon}_{\mathrm{m}}) = \frac{\tilde{\varepsilon}'_p - \tilde{\varepsilon}_{\mathrm{m}}}{\tilde{\varepsilon}'_p + 2\tilde{\varepsilon}_{\mathrm{m}}} \tag{19}$$

where $\tilde{\varepsilon}'_{\mathrm{p}}$ is defined as [102]

$$\tilde{\varepsilon}'_p(\tilde{\varepsilon}_1, \tilde{\varepsilon}_2) = \tilde{\varepsilon}_1 \left[\frac{\left(\frac{R_1}{R_2}\right)^3 + 2\left(\frac{\tilde{\varepsilon}_2 - \tilde{\varepsilon}_1}{\tilde{\varepsilon}_2 + 2\tilde{\varepsilon}_1}\right)}{\left(\frac{R_1}{R2}\right)^3 - \left(\frac{\tilde{\varepsilon}_2 - \tilde{\varepsilon}_1}{\tilde{\varepsilon}_2 + 2\tilde{\varepsilon}_1}\right)} \right] \tag{20}$$

Single-shell model can be extended to multiple shells to model more complex cell structures such as cells with a surrounding cell wall [104]. These walled structures are typical for plant cells as well as for many important single-cell microorganisms such as yeast cells and bacteria [104].

A typical mammalian cell consists of a highly conducting cytoplasm surrounded by an insulating membrane, which is known as protoplast model [104]. Therefore, effective dipole moment of a mammalian cell can be modeled adequately by using the singe-shell model [118]. The dielectric properties of the cells can be measured by using the method of electrorotation (ROT), time domain dielectric spectroscopy (TDDS) [119] or single-cell dielectric spectroscopy [120]. Among these ROT is a well-developed and commonly used method to obtain the dielectric properties of the cells. In this method, the rotation of the cells resulting from the torque induced by an applied rotating electric field is measured as a function of field frequency. To provide estimates for the dielectric properties of the cells, the parameters of the single-shell [121] or multi-shell [122] model are optimized to fit the experimental ROT spectrum data (ROT spectra can also be used for the determination of viability of parasites [123]). Using the estimated properties, DEP spectra of the cells can be determined. Figure 5 shows the DEP spectra of a two-layered spherical particle with some representative values for the dielectric properties of mammalian cells for different medium electrical conductivities. Different from the homogeneous particle, two cross-over frequencies exist. The first cross-over frequency is a strong function of the medium conductivity, and with increasing conductivity, the cross-over frequency shifts to higher frequency values. The first cross-over frequency is also a function of the permittivity of the membrane (i.e. membrane capacitance). To demonstrate this effect, the case with different membrane permittivities is also included in the figure with dashed line. As the permittivity of the membrane decreases, the cross-over frequency shifts to higher frequency values.

Some biological particles cannot be simply described as sphere. They can be modeled as ellipsoids, cylinders and rods. To determine the dipole moment expression and the corresponding DEP force expression, the calculation of the electrical potential around the particle is required. For simple spherical, ellipsoidal particles (prolate and obsolete ellipsoids are the special cases of ellipsoid), the analytical solutions are available [102, 104, 124, 125]. However, for geometries other than sphere and ellipsoids, such as cylinders and rods, numerical solutions are required to determine the electrical potential around particles, dipole and multipolar moments [126–128].

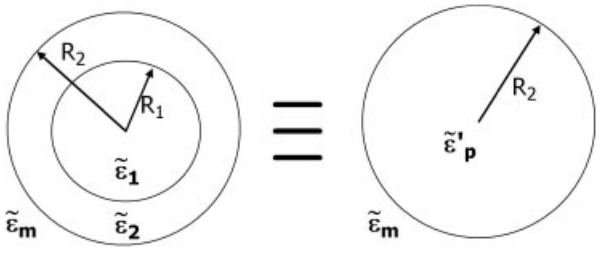

Figure 4. Schematic illustration of the single-shell model.

3 Simulation of particle motion in microchannels for DEP applications

In the design of microfluidic systems for the manipulation of particles, simulation (or numerical prototyping) is an

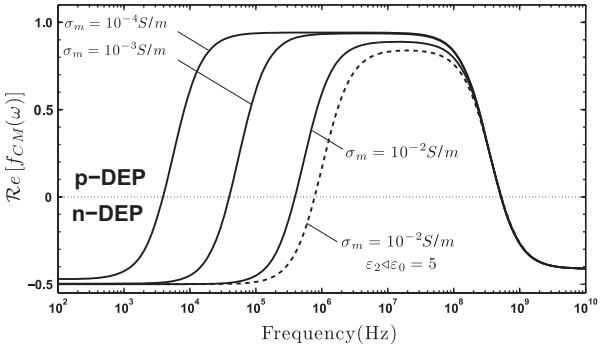

Figure 5. DEP spectra of a spherical particle with single-shell for different medium conductivities: $R_1 = 2.01\,\mu\mathrm{m}$, $R_2 = 2\,\mu\mathrm{m}$, $\varepsilon_{\mathrm{m}}/\varepsilon_o = 80$, $\varepsilon_1/\varepsilon_o = 10$, $\varepsilon_2/\varepsilon_o = 60$, $\sigma_1 = 10^{-8}\,\mathrm{S/m}$, $\sigma_2 = 0.5\,\mathrm{S/m}$, $\sigma_{\mathrm{m}} = 10^{-4}$, 10^{-3}, $10^{-2}\,\mathrm{S/m}$.

important step in order to determine the most feasible and optimum geometry of the electrodes and the microchannel network. Performing the simulations, the predictions of the trajectories of the particles are very crucial. Since the trajectory of the particles is a result of the interaction of the particles with the fields, corresponding field variables need to be determined. For the DEP applications in microfluidics, the electrical potential field, the flow field and the temperature field (if appreciable temperature gradients are present) need to be considered.

The governing equation for the electric potential inside an LOC device is Laplace's equation as

$$\nabla \cdot [(\sigma + i\omega\varepsilon)\nabla\phi] = 0 \tag{21}$$

since the convection of the transport of the ions are negligible due to low convection nature of the microfluidic applications. If there is no significant variation of conductivity and permittivity, Eq. (21) can be reduced to Laplace's equation ($\nabla^2\phi = 0$). Considering the thin-double-layer assumption, the boundary conditions are predefined voltages on the electrode surfaces, and insulation on the channel walls (since there is a large difference between the permittivities and the conductivities of the water and the channel material which is most of the time either glass or polymer-based material). At the inlet and exit of the channel, either periodic boundary condition can be used if the computational domain is repeating itself or insulation boundary condition can be used if the inlet and the exit are sufficiently far away from the electrodes. Predefined voltages on the electrode surfaces is a reasonable approach in the case of a DC field (where $\omega = 0$), and reasonable approach for high-frequency applications compared to the charge-relation frequency ($\omega > 100$ kHz for a solution with a conductivity of 0.001 S/m), which is typical for microfluidic applications. If this criterion is not satisfied, the following mixed-type boundary conditions need to be implemented on the electrode surface

$$\phi - \frac{\sigma}{i\omega C}\frac{\partial\phi}{\partial n} = V_o \tag{22}$$

where V_o is the predefined voltage at the electrode, C is the double-layer capacitance which is given by the ratio of the electrolyte permittivity to the Debye length ($C \sim \varepsilon/\lambda_D$).

The governing equation for the flow field is the incompressible Navier–Stokes equation together with the continuity equation as

$$\nabla \cdot \mathbf{u} = 0 \tag{23}$$

$$\rho(\mathbf{u}\cdot\nabla)\mathbf{u} = -\nabla P + \mu\nabla^2\mathbf{u} + (\rho - \rho_o)g \tag{24}$$

where ρ and μ are the density and the viscosity of the bulk liquid. ρ_o is the density of the fluid at room temperature. The boundary conditions for the flow field can be predefined pressures at the inlet and the exit (zero pressure can be assigned for the exit) of the microchannel if the flow is pressure driven, or uniform inlet velocity corresponds to the desired volumetric flow rate of the fluid. At the walls and the electrodes, the normal velocity will be zero. The common pratice for DC-DEP application is the use of external electrodes, and the voltage is applied across the length of the device. Therefore, flow is generated by the applied electric field (i.e. EOF). If the flow is EOF together with the thin-double-layer assumption, slip velocity can be assigned at the walls as

$$u_{\text{slip}} = \mu_{\text{EO}}(\nabla\phi)_t \tag{25}$$

where μ_{EO} is the electro-osmotic mobility. The common practice for the AC-DEP applications is to use internal electrodes, then no-slip boundary condition is assigned on each boundary. In the case of AC-electroosmosis, slip velocity on the electrodes needs to be assigned [129].

The second term of Eq. (24) is the inertia term. For the flow inside micron-scale channels, the Reynolds number ($Re = \rho UL/\mu$) which is the dimensionless number showing the ratio of inertia forces to viscous forces is small, in the order of 10^{-2}, therefore inertia term can be neglected, and instead of solving non-linear Navier–Stokes equation, linear Stoke's equation can be solved.

If the significant temperature gradients exist inside the device, the energy equation also need to be solved to get the temperature field. If the temperature variation in the system is appreciable, then all the equations become coupled since the thermophysical properties such as ε, σ, ρ, μ, C_p and k have temperature dependence. However, the temperature rise via Joule heating or external sources is not favorable because it may disrupt the operation of the device. Moreover, if the device is for the manipulation of in vivo cells, the heating should be avoided since in vivo cells cannot tolerate dramatic temperature rise. Therefore, microfluidic devices are aimed at operating without any appreciable temperature rise. Temperature rise can be estimated by using Eq. (8). For AC-DEP applications, it is typical that temperature rise is in acceptable limits (<10 K) unless the electrical conductivity of the solution is high, say >1 S/m. However, it can be an issue for DC-DEP applications. In this case, the energy equation needs to be solved both for the microfluidic channel and for the surrounding LOC device. Summary of the governing equations and boundary conditions for typical DC-DEP and AC-DEP applications are given in Fig. 6.

Particle trajectory is the result of the interaction of the particle with the electric field and the flow field. To simulate the particle trajectories, there are two approaches. The first approach is to treat the particles as point particles, and solve the field variables without the presence of the particles. In this case, the effect of the particle on the field variables is ignored, only the effect of the field variables on the particle is considered. The particle trajectories can be obtained at the post-processing step of the numerical computation. In the second approach, the field variables are solved with the presence of the finite-sized particle, and the particle is moved as a result of this interaction. In each incremental movement of the particle, the field variables need to be resolved. The former approach is very simple and works good to some extent, latter approach is accurate; yet, computationally expensive. Both approaches, point particle [8, 9, 12, 14–16, 45, 49, 64–68, 93, 96, 130, 131] and finite-sized particle [109, 132–136] have been performed to

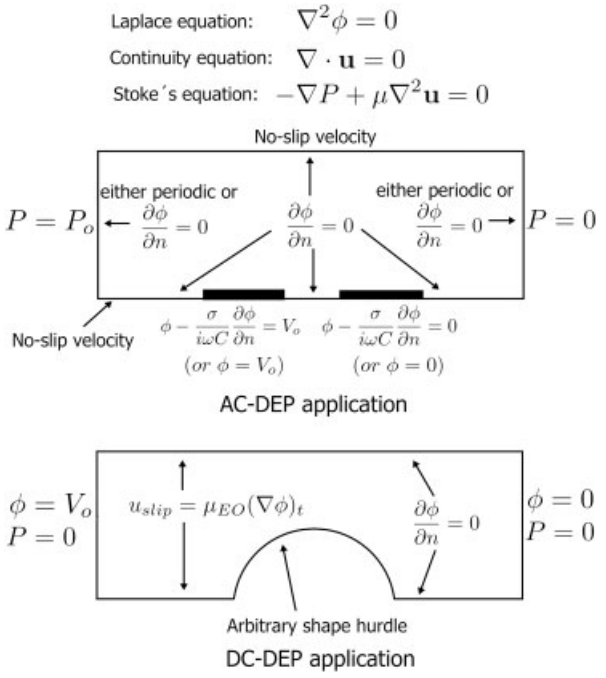

Figure 6. Governing equations and boundary conditions for typical DC-DEP and AC-DEP applications.

simulate the particle trajectory for the DEP applications. Both approaches will be discussed in detail.

3.1 Point-particle approach

In this approach, particles are assumed to be point particles, and the effect of the particle on the field variables is ignored, only the effect of the field variables on the particle is considered. The field variables are determined without the presence of the particles. Together with the following assumptions:

(i) the thermophysical properties of the liquid are constant and there is no thermal effect on flow field and particle velocity,
(ii) the particle and the channel walls are non-porous, and do not react with the surrounding liquid,
(iii) the rotation of the particle does not affect the particle's translation motion,
(iv) creeping flow (i.e. $\mathrm{Re} = \rho U_{\mathrm{mean}} L/\mu \approx (1000\ \mathrm{kg/s}) \times (10^{-4}\ \mathrm{m/s}) \times (10^{-4}\ \mathrm{m})/(10^{-3}\ \mathrm{kg/ms}) = 0.01 \ll 1$),
(v) the solution is dilute enough to neglect the electrostatic interaction between the particles, the particle position $\mathbf{x_p}$ can be determined, by integrating the particle velocity together with the initial position

$$\mathbf{x}_{\mathrm{p}}(t) = \mathbf{x_o} + \int_0^t \mathbf{u}_{\mathrm{p}}(\tau)\, \mathrm{d}\tau \tag{26}$$

where $\mathbf{x_o}$ is the initial position of the particle, and t is the time.

For a fixed frame of reference, the translational motion of a particle is governed by

$$m_{\mathrm{p}} \frac{\mathrm{d}\mathbf{u}_{\mathrm{p}}}{\mathrm{d}t} = \mathbf{F}_{\mathrm{ext}} \tag{27}$$

where m_{p} is the particle mass and $\mathbf{F}_{\mathrm{ext}}$ is the net external force. The drag force on a spherical particle is given by

$$\mathbf{F}_{\mathrm{drag}} = 6\pi\mu R(\mathbf{u} - \mathbf{u}_{\mathrm{p}}) \tag{28}$$

at the creeping-flow limit, which is known as Stoke's law [137], where R is the particle radius, $\mathbf{u}$ is the fluid velocity, $\mathbf{u}_{\mathrm{p}}$ is the particle velocity.

The DEP force acting on a spherical particle is given by Eq. (13). For the particle size considered in this study, the characteristic time scale of acceleration period of the motion is in the order of 10^{-4} s [8, 111] which is much smaller than the time scale of the variation of the field variables. Therefore, the acceleration term can be safely neglected. It can be assumed that the particles move with the terminal speed at all times. Substituting Eqs. (13) and (28) into Eq. (27), the particle velocity can be obtained as

$$\mathbf{u}_{\mathrm{p}} = \mathbf{u} - \frac{\varepsilon_{\mathrm{m}} R^2 \mathrm{Re}[f_{\mathrm{CM}}(\omega)]}{3\mu} \nabla \mathbf{E}_{\mathrm{rms}}^2 \tag{29}$$

The trajectories of the particles can easily be obtained as a streamline plot, once the x- and y-component of the above equation are introduced as the x- and y-component of the stream function.

This approach is very simple; however, has some limitations. Eq. (29) is valid if the particle size is small compared to the device dimensions, and it is valid for spherical particles. (It can be modified for ellipsoid particles [86]). Sometimes these limitations are strong to apply this approach. However, there are some modifications that can be implemented to expand the validity of this approach. When the electric field variation is too strong (e.g. when large particles are moving close to the electrodes), higher order moments can be introduced for the determination of the DEP force. For Stoke's law to be valid, the particle needs to be several diameter away from the solid boundaries and the other particles. To take these complication into account, an empirical correction factor (C) can be introduced into Eq. (29) as

$$\mathbf{u}_{\mathrm{p}} = \mathbf{u} - C\frac{\varepsilon_{\mathrm{m}} R^2 \mathrm{Re}[f_{\mathrm{CM}}(\omega)]}{3\mu} \nabla \mathbf{E}_{\mathrm{rms}}^2 \tag{30}$$

It is expected that for small particles, the correction factor approaches to unity, and for larger particles, it is between 0 and 1.0 depending on the size of the particle and the microchannel, and needs to be determined experimentally. Due to this, point-particle approach is not accepted as a rigorous method to model the particle trajectory inside LOC devices. This approach has been implemented successfully for the prediction of the particle trajectories inside the microchannels [8, 9, 64–67, 93, 130].

If the particle size is <1 μm, the Brownian motion can be effective. If the Brownian motion is not strong enough, the particle trajectory can be superimposed by deterministic

trajectory and probabilistic trajectory. In this case, a transient force that represents the Brownian forces as an additional external force can be implemented to Eq. (27) [138].

If an external DC-field is applied across the channel, for a particle with surface charge, EP motion needs to be considered also. In this case, EP contribution can be included in Eq. (29) as $\mu_p\mathbf{E}$ in which μ_p is the electrophoretic mobility of the particle and defined as, $\mu_p = \varepsilon_f\zeta_p/\mu$, where ε_f is the permittivity of the fluid, ζ_p is the ζ potential of the particle, μ is the viscosity of the fluid [8, 9, 12, 14–16, 93, 96]. When the particle moves close to the wall, there is electrical and hydrodynamic interaction between the particle and the wall. This interaction of the particle and the wall can also be implemented as an empirical relation in Eq. (29) [8].

3.2 Finite-sized particle approach

In this approach, the field variables are determined with the presence of the finite particle size. The trajectory of the particles can be determined accurately without defining any empirical parameter that makes this method as a rigorous method to model the particle trajectory inside LOC devices. The resultant forces on the particle can be determined by integrating the corresponding stresses over the particle surface. In this approach, particle may have any arbitrary shape. If the temperature variation is insignificant, only the flow field and the electric field needs to be determined. The resultant drag force can be determined by integrating the hydrodynamic stress tensor [109], and the resultant DEP force can be determined by integrating the MST, Eq. (3) [109, 139]. In this approach, there is no need to define a CM factor. The resultant torque on the particle can also be determined and the rotation of the particle can also be included in the analysis unlike the point-particle approach. The translational velocity and the rotational velocity of the particle can be determined by solving the conservation of linear and angular momentum equation for the particle. Trajectory and the angular orientation of the particle can be obtained by integrating the translational and angular velocity of the particle over the time. The drawback of this method is that it is computationally expensive. As the particle moves in the microchannel, the meshes need to be updated from time-to-time. However, by using commercial softwares like COMSOL Multiphysics®, the procedure can be automized, and with a powerful desktop computer, these kinds of computations can be performed in a feasible manner. This approach has also been implemented for the prediction of the particles inside microchannels for both spherical [109, 132–135] and cylindrical particles [136].

Our discussion of dielectrophoresis is limited to very dilute suspensions whose behavior is mainly governed by the interaction of a particle with an external electric field. However, when the particles are packed, there exists strong electrical and hydrodynamic interaction between the particles which strongly affects the trajectory and the motion of the particles in the microchannels [140–142]. Even though the solution is dilute enough, these interactions come into picture when particles accumulate at specified locations (e.g. concentration and trapping processes). Moreover, when particle moves close to the wall, there also exists particle–wall interaction. All these complications can be modeled with finite-sized particle approach without introducing any empirical parameter [132–136]. However, when the number of particles is large, the modeling is not computationally feasible using finite-sized particle approach. Park and Saintillan [140, 141] proposed an efficient computational algorithm to simulate the characteristics of large-scale suspensions of ideally polarizable (e.g. conducting) spheres under the action of electrokinetic forces. They were able to simulate a suspension consists of 2000 particles with a volume fraction of 20%. An alternative approach to model electrolyte solutions with large number of particles (colloidal suspensions) is to define concentration-dependent density and viscosity for the suspension, and model the liquid–particle mixture as a single-phase liquid [143].

4 Applications of DEP in microfluidics

Manipulation of biological particles is a very important task and demanded in many chemical, biological and biomedical applications. A label-free method like DEP is very attractive to manipulate biological particles. Therefore, DEP has been implemented for many applications regarding the manipulation of particles such as separation, focusing, sorting, trapping, concentrating, filtering and patterning of microparticles, cells, biological particles and nanoparticles inside microfluidic devices. The DEP-based microfluidic methods and devices, which are proposed to handle these operations, are discussed in this section. As seen from Eq. (13), DEP has the potential to separate particles according to their size and according to their electrical properties if non-uniform electric field is present inside the device. The main idea is to curve the electric field lines inside the microfluidic channel. This can be achieved by designing insulating hurdles (or posts) inside the microchannel network (iDEP applications, see Fig. 7A), fabricating different electrode geometries inside the device (see Fig. 7B) or by designing curved microfluidic channels.

For iDEP applications, since the electric fields are generated by means of electrodes at the inlet and exit reservoirs, high voltages are needed. Therefore, DC-field or low-frequency AC-field is preferred due to practical difficulties to generate high AC voltages with high frequency. When DC field is used, flow is also induced by the applied DC electric field (i.e. EOF). Therefore, flow field and DEP force field are coupled, and both depend on the applied voltage at the reservoirs. This diminishes the flexibility of the system; however, it is advantageous since there is only one control parameter which is the voltage. For DC-DEP applications, the CM factor depends on the conductivity of the particle and the medium. Polystyrene particles usually exhibit n-DEP, only polystyrene particles with small

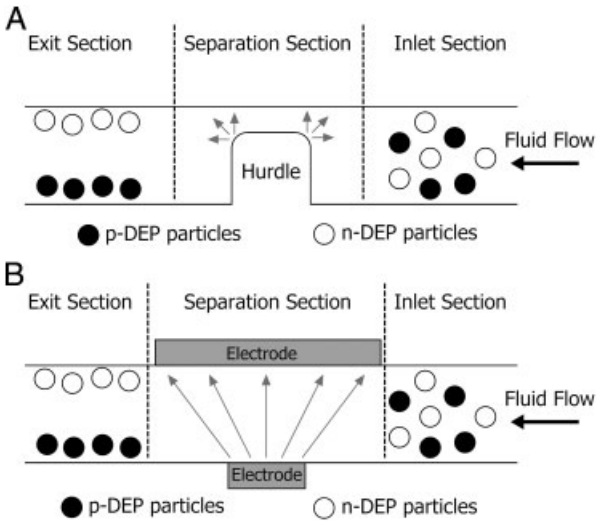

Figure 7. Schematic drawing of DEP-based microfluidics devices: (A) non-uniform electric field by means of insulating hurdle, (B) non-uniform electric field by means of asymmetric electrodes (gray arrows represents the direction of the n-DEP force).

diameter can exhibit p-DEP in a low-conductivity buffer solution (e.g. deionized water). On the other hand, live cells [4–6] only exhibit n-DEP response in DC-field. DC-DEP is a perfect match for separation by size applications. Barbulovic-Nad et al. [7] introduced a circular oil droplet as an insulating hurdle inside the straight channel and separated 1, 5.7 and 15.7 μm polystyrene particles. Kang et al. [6, 8, 9] introduced rectangular insulating hurdle in a straight microchannel to separate polystyrene particles by size, see Fig. 8A. One major disadvantage was the strong electric field experienced by the particles as passing through the narrow region. In order to avoid the effect of narrow region, same group offered the use of triangular hurdle for the separation of white blood cells and breast cancer cells by their size [6] as shown in Fig. 8B. Lapizco-Encinas et al. [4] introduces circular posts to separate different bacteria species, namely Gram-negative *Escherichia coli* and the Gram-positive *Bacillus subtilis*, *B. cereus* and *B. megaterium* (see Fig. 8C and D). Using iDEP together with DC-field, trapping and concentration of bacteria cells from a mixture with 0.2–1 μm polystyrene particles [5], concentration of linear-DNA [10], concentration of *E. coli* and *S. cerevisiae* cells [11], focusing of polystyrene particles [12] and concentration of 500 nm–1 μm nanoparticles [13] are utilized inside LOC devices. Although cells have n-DEP response in a DC field, viable and non-viable cells may have different CM factors, and cells can also be separated according to their states in a DC field [4].

For iDEP applications, the flow field and DEP force field can become independent by applying DC-biased AC fields. In this case, DC field induce the EOF, and the combination of AC and DC fields can contribute to the DEP force field, and at low-frequency limit (<10 kHz) the contribution of both fields on the CM factor is the same. Since electrodes are submerged into the reservoirs for iDEP applications, in order to get an efficient DEP force from an AC-field, the applied voltage needs to be high. Typical function generators supply 20 V_{p-p}. Higher voltages can be achieved by function generators that operate at low frequency, or by connecting the function generator to a power amplifier. iDEP together with DC-biased AC-field is utilized to separate polystyrene particles by size [91–93], to trap chromosomal DNA from lysed *E. coli* cells [94], to sort blood cells and *E. coli*, to trap and concentrate single- and double-stranded DNA molecules [95], to filter *E. coli* from yeast cells [96], to trap linear and supercoiled DNA molecules [97]. Cardiel et al. [98] utilized high-AC voltage with a very low frequency (~1 Hz) in an iDEP device to trap 1 μm polystyrene particles and move them in bands in a highly controlled manner. AC-field together with pressure-driven flow can also be utilized for iDEP applications with the inclusion of a power amplifier to the system. Focusing of polystyrene particles and viable HeLa cells [99] was achieved by introducing funnel-shaped insulating structures.

Instead of using insulating structures, Zhu et al. [16] proposed the use of spiral-shaped microchannel to generate non-uniform electric field, and was able to separate 3, 5 and 10 μm polystyrene particles.

Non-uniform electric field inside an LOC device can be induced by using specially designed planar electrode geometries embedded inside the device (deposited either at the bottom wall, or both bottom and top wall). In order to avoid ion accumulation at the electrodes, AC-field is the only option for internal electrodes. Since the electrodes are in the device, low-voltage values are enough to generate sufficient DEP force which can be generated by a conventional function generator frequency ranging from tens of kHz to tens of MHz. For DEP applications with internal electrodes, flow is generated by means of pressure difference between inlet and exit reservoirs. It is more flexible, since flow and the DEP force field can be adjusted independently, paybacks are an additional control parameter which is the applied pressure at the reservoirs, and additional components such as syringe pumps. In the case of AC-field, CM factor is also a function of the frequency of the electric field. Switching the frequency of the field, either n-DEP or p-DEP response is possible. DEP force is proportional to particle volume and electrical properties of the particle and the medium. Each cell has a distinct morphology, and hence has a distinct dielectric signature which is a function of cell type, cytoplasmic complexity, cell cycle phase and cell viability. This unique dielectric signature can be utilized to discriminate and identify cells from the other particles or to detect and isolate diseased or damaged cells by means of AC-DEP (DEP force spectra of different cell types can be found elsewhere [118, 144]). AC-DEP has been implemented for the separation of cancer cells from blood stream [17, 18], the separation of red blood cells and polystyrene particles [19], the separation of human leukocytes [20], the isolation of the malaria-infected cells from the blood [21, 22], the separation of the electroporated and non-electroporated cells [23], the

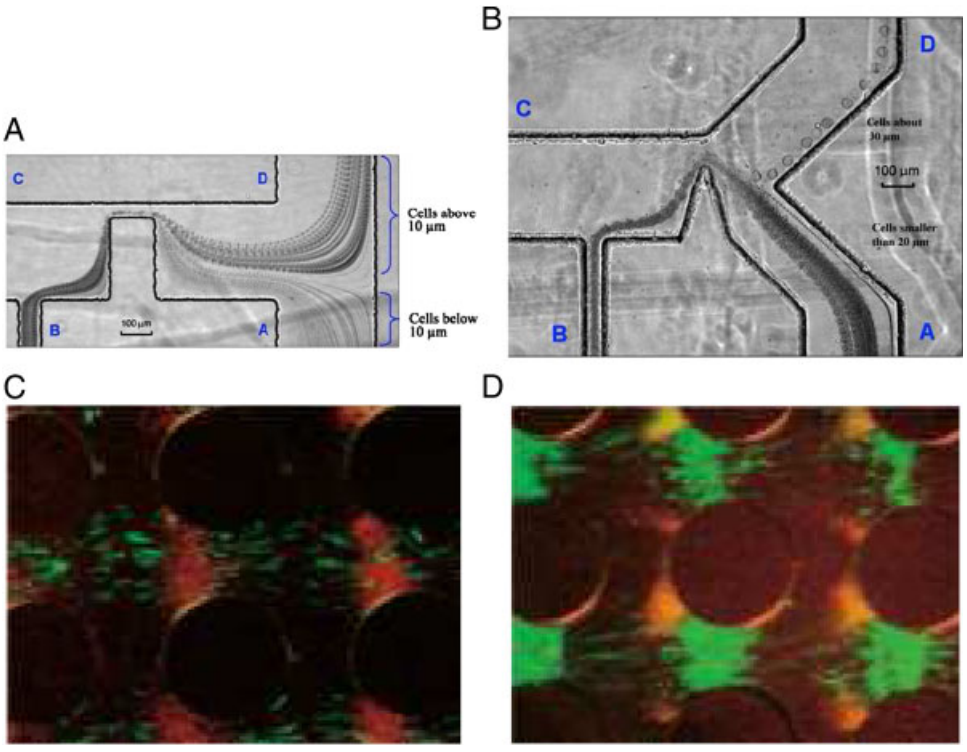

Figure 8. (A) Separation of white bloods cells by size using rectangular hurdle (Reprinted with permission from Ref. [6], copyright 2008 Springer), (B) separation of breast cancer cells by using triangular hurdle (Reprinted with permission from Ref. [6], copyright 2008 Springer), (C) selective trapping of *B. cereus* [4], (D) selective trapping of *B. subtilis* [4].

separation of the platelets from diluted whole blood [24], the separation of red blood cells and the white blood cells [25], the separation [26–28] and sorting [29] of viable and non-viable yeast cells, the separation of healthy and unhealthy oocyte cells [30], the characterization and the sorting stem cells and their differentiated progeny [31], the isolation of rare cells from biological fluids [32], the separation of three distinct bacterial clones of commonly used *E. coli* MC1061 strain [33], trapping of viable mammalian fibroplast cells [34], trapping of DNA molecules [35], trapping of single cancer and endothelial cells to investigate pairwise cell interactions [36], trapping of bacterial cells for the subsequent electrodisruption or electroporation [37], focusing of polystyrene particles [38], trapping of yeast cells [39], 3-D focusing of polystyrene particles and yeast cells [40], the separation of airborne bacterium, *Micrococcus luteus*, from a mixture with dust and polystyrene beads [41], trapping and isolation of human stem cell from heterogeneous solution [42], single-cell isolation [43], concentration and counting of polystyrene particles [44], the separation of polystyrene particles, Jurkat cells and HeLa cells [45], the separation of viable and non-viable mouse-hybridoma 3-2H3 cells [46] and the separation of colorectal cancer cells from other biological materials [47]. Separation by size [48–50] can also be implemented for AC-DEP applications. Among the separation and sorting devices, some of them require discrete processes (i.e. trap and rinse) [4, 5, 17–20, 23, 25, 27, 28, 30, 48, 61, 73, 95], and some of them are continuous-flow devices [24, 26, 33, 41, 45–47, 52, 55, 63, 67, 67]. The processes regarding the manipulation of particles can be integrated for the rapid and automated analysis of biological samples [118, 145, 146]. In this case, continuous-flow devices are more suitable for sequential integration of separation with other operations. Krishnan et al. [51] utilized AC-DEP together with magnetophoresis to trap different-sized beads at different locations inside microchannel.

Although separation by size was achieved by either DC-DEP or AC-DEP, the main issue is that in order to have a successful separation by size, the size difference of the particles needs to be large (i.e. separation of 5 and 6 μm is problematic). However, by AC-DEP, separation by properties is possible. On the other hand, deterministic lateral displacement devices offers a fine tuning for separation by size; however, fails in separation by properties. Beech et al. [52] proposed a hybrid system that utilizes deterministic lateral displacement and DEP to improve the size resolution and possible separation by electrical properties.

Use of planar electrodes can be problematic due to adhesion of the particles on the electrode surface or on the channel wall. This issue can be avoided by fabricating planar electrodes both on the bottom and the top wall of the channel. In that case, the particles can be focused and located around the center of the channel in the height direction. This kind of electrode configuration has been proposed for the focusing of polystyrene particles and leukemia cells for cytometry applications [53], the capturing of microparticles for immunoassaying [54], for the separation of 9.6 and 16 μm polystyrene particles [48], and for the separation of red blood cells, bacteria and liposomes using twDEP [55]. On the other hand, the adhesion of the particles on the channel wall can be favorable for some other applications like cell patterning for tissue engineering [56].

Hsiung et al. [57] designed planar ring electrodes to pattern human hepatocellular carcinoma cells. They achieved highly uniform patterning over the array of electrodes. Suzuki et al. [58] patterned two different cell types without any special pretreatment of a culture slide on a microelectrode array fabricated with indium-oxide. Park et al. [59] presented a DEP-based device with reusable electrodes on a printed circuit board for patterning cervical cancer cells and polystyrene particles. Reusable electrodes make this device very cost-effective and convenient for rapid prototyping. More recently, Tsutsui et al. [60] developed a microfluidic platform with an embedded array of microwell structures to achieve viable and homogeneous monolayer patterns for mouse embryonic stem cells by p-DEP.

One major issue is the throughput of the DEP-based devices. Their throughput is low compared with other conventional manipulation techniques [108]. One way to increase the throughput is to increase the channel dimensions. For the devices with planar, internal electrodes, the height of the device can not be increased, since there is a confined region over the electrodes where the DEP force is effective (DEP force decreases drastically in the height direction). The particle needs to flow in the vicinity of this confined region. For trapping devices, the width of the channel can be increased to increase the throughput; however, this is not a solution for continuous-flow devices. One alternative is to solve this problem by using 3-D electrodes at the sidewalls. In this case, DEP force in the height direction remains the same; however, 3-D electrodes introduce an additional complexity in the fabrication process. Iliescu et al. [147] proposed to use of highly doped silicon as an electrode and fabricate a 3-D electrodes, and managed to separate viable and non-viable yeast cells [61]. Wang et al. [148] proposed the fabrication of 3-D electrodes at the sidewalls by electroplating, and utilized this structure for flow cytometry [62] and continuous separation of human-kidney cells and N115 mouse-neuroblastoma cells by AC-DEP [63]. Kang et al. [64], and Cetin et al. [65, 67] fabricated 3-D copper electrodes with an extended-photolithography technique and embedded them along the sidewalls to implement for the continuous separation of polystyrene particles and cells by size [64, 65] and by electrical properties [67] (see Fig. 9A and B). Demierre et al. [68] proposed a use of a side channels (what they called access channels) filled with buffer solution and in touch with the electrodes to shape the electric field in 3-D without any need for an additional 3-D electrode fabrication step. They utilized the focusing of microparticles [68], and sorting of viable and non-viable yeast cells [69, 70] by this design. Duarte et al. [71] and Jaramillo et al. [72] proposed the use of 3-D carbon electrodes which are fabricated by C-MEMS technique for superior filtering efficiency. Use of carbon electrodes also minimized the possibility of electrolysis since carbon is chemically more stable than metals. They successfully trapped yeast cells from the mixture with polystyrene particles [71], and *E. coli* bacteria from a mixture with *B. cereus* bacteria [72]. In the former one, instead of conventional syringe pumps, centrifugal pumping is utilized by means of a compact-disk-based centrifugal platform. Lewpiriyawong et al. [49] proposed the use of conductive PDMS as 3-D sidewall electrodes, and utilized AC-DEP for the continuous separation of 10 and 15 μm polystyrene particles. The PDMS was mixed with gold-powder to make PDMS conductive. Shafiee et al. [73] proposed to use side channels which are separated from the main channel by a 20-μm-thick PDMS barrier (what they call contactless DEP). By applying the AC-field through the electrodes submerged in the reservoirs of the side channels, the electric field lines penetrated through the thin PDMS and non-uniform electric field was obtained in the channel. They utilized AC-field for the separation of human leukemia cells from dead cells [73]. For many of the DEP base devices, the electric field is experienced throughout the device. The interaction of the live cells can be undesired, if the cells will be processed later, One possible solution of this can be the use of local electric fields to manipulate particles. Electrodes that will generate 3-D DEP force field in the transverse direction to the flow also offers local electric fields [49, 64, 65, 67–70, 73]. Another alternative to increase the throughput of the continuous-flow systems is to utilize twDEP by using planar electro-arrays for the manipulation of particles [55, 74]. Simple increasing the width of the channel will lead to high throughput. Increasing the width of the channels may increase the resistance of the electrodes due to the increased length; however, this issue can be solved by using some appropriate design of the electrodes and the location of the electrical connections. Choi et al. [74] proposed a multilayered bus-bar design to maintain low resistance in microelectrodes for increasing device are, and demonstrated the high-throughput separation of 3, 6, 10 and 20 μm polystyrene particles.

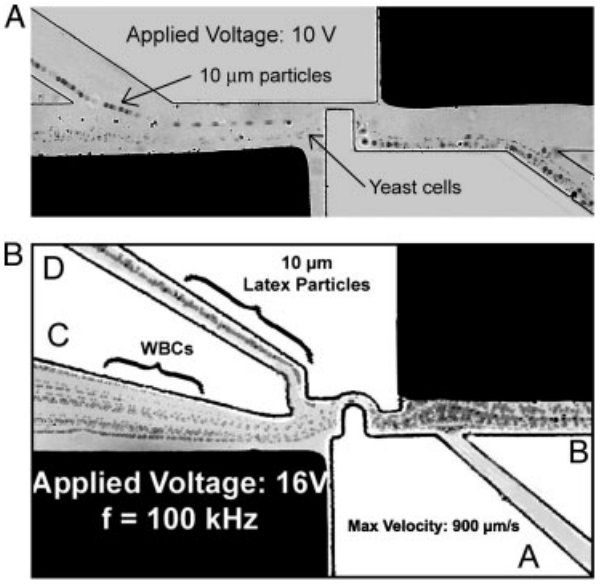

Figure 9. (A) Separation of white blood cells and yeast cells (Reprinted with permission from Ref. [64], copyright 2009 Elsevier), and (B) separation of white blood cells and 10 μm latex particles [67].

Table 1. Summary of manipulation of microparticles with DEP

Operation	Type of particles	References
Separation by size	Polystrene particles	[7–9, 16, 48–50, 52, 64, 65, 91–93]
	Cells	[5, 6, 55, 64, 65]
Separation by properties (trap and rinse)	Cells	[4, 5, 17–20, 23, 25, 27, 28, 30, 48, 61, 73, 95]
	Nanoparticles	[80, 84]
Separation by properties (continuous flow)	Polystrene particles	[52, 67]
	Cells	[24, 26, 33, 41, 45–47, 55, 63, 67]
	Nanoparticles	[81, 82]
Concentration	Polystrene particles	[44]
	Cells and biological particles	[10, 11, 21, 22, 95]
	Nanoparticles	[13, 80]
Focusing	Polystrene particles	[12, 16, 38, 53, 68]
	Cells	[40, 96, 99]
Sorting	Polystrene particles	[74, 75]
	Silica particles	[79]
	Cells	[29, 31, 55, 69, 70]
Trapping	Polystyrene particles	[98]
	Cells and biological particles	[34–37, 39, 42, 43, 54, 71, 72, 94, 95, 97]
	Carbon nanotubes	[85]
	Nanospheres	[78]
	Magnetic beads	[51]
Filtering	Cells	[32, 96]
	Multi-walled carbon nanotubes	[83]
	Nanospheres	[78]
Patterning	Cells	[56–60]
	Carbon nanotubes	[85–90]

Although DEP response of particles can be tuned by changing the permittivity and the conductivity of the medium theoretically, in practice, especially when working with cells and biological particles, this is not possible because there are certain limitations about the buffer solution in which the biological particles are placed in. These buffer solutions are highly conductive most of the time. It is hard to get a p-DEP response from the particles suspended in a highly conductive solution. The particles tend to show n-DEP response for the entire frequency spectrum. Therefore, there is a medium conductivity limit which both p-DEP and n-DEP response is present. Khoshmanesh et al. [75] proposed to coat the biological particles with carbon nanotubes (CNTs), which enables to get both p-DEP and n-DEP responses at higher medium conductivities. They also demonstrated that if the electrodes are patterned with CNTs, the DEP force field become stronger due to the strong local DEP force fields generated at the tip of the patterned CNTs. However, once the particles are coated with CNTs, then DEP cannot be called as label-free, and the removal of the CNTs form the particles can be an unachievable process if desired.

Although DEP force decreases with size, very high electric field strengths can be achieved by fabricating electrodes with very small spacing which enables manipulation of viruses [76, 77] and nanoparticles with DEP. iDEP together with DC-field was used to filter and trap 200 nm nanoparticles [78], and AC-DEP has been utilized for the concentrated 250 nm silica nanoparticles to establish a particle-core/liquid-cladding optical waveguide [79] and the separation and detection of DNA-derivatized nanoparticles [80]. Manipulation of nanoparticles such as CNT, peptide nanotubes (PNT) and nanoparticles is also very important for the development of the bionano/nanotechnology-based devices and nanomaterial-based sensors, and has attract recent attention by the DEP community. Today's synthesis techniques produces heterogeneous mixture of semiconducting, semimetallic and metallic single-walled CNTs [81], and all these kinds have different application areas. Therefore, separation and purification of specific kind single-walled CNTs is very crucial. Shin et al. [81, 82] utilized AC-DEP for the separation of metallic single-walled CNTs and the semiconducting single-walled CNTs. Wei et al. [83] utilized AC-DEP for the removal of the impurities and increase the purity of the CNTs. Zhang et al. [84] separated multi-walled CNT and 1 μm polystyrene particles in a trap and rinse manner. Patterning of nanotubes and nanoparticles are very crucial to construct nanostructures in desired configuration. Nanoparticles and nanotubes can be immobilized in certain configuration using specially designed electrode structures by utilizing p-DEP force for trapping. CNTs are sensitive to oxidative or reducing gases, and their electrical conductance effected by the level of presence of such gases [85]. This makes CNTs as a perfect match for sensor applications. Xu et al. [86] studied the mechanism of manipulating CNTs for different electrode geometries, and analyzed the motion of the CNTs numerically

and experimentally. Xu et al. [87] also presented the use of floating electrodes for high-precision alignment of CNTs over the electrodes. Ferrara et al. [88] proposed a system that patterns nanowires using palladium nanoparticles. It was illustrated that the conductivity of nanowires are sensitive to hydrogen content, and the proposed is suitable to be a hydrogen sensor. Suehiro et al. [85] utilized the DEP-trapped CNTs as gas sensors to detect NO_2 and NH_3. They also trapped *E. coli* on a microelectrode by the help of multi-walled CNTs attached to the end of the microelectrodes. Lee et al. [89] proposed the use of virtual electrodes generated by programmed light patterns to manipulate CNTs which enable several electrode configurations in a single device which normally would require the fabrication of each electrode configuration separately. Likewise CNTs, DEP patterning was also utilized to assemble bionanostructures. Castillo et al. [90] immobilized amyloid PNT on top of gold microelectrodes, and were able to measure the electrical properties of the patterned nanotubes. Assembly of such peptide-based nanotubes has a high potential for bionanotechnology applications. Applications regarding the manipulation of micro/nanoparticles with DEP is summarized in Table 1 (different kinds of biological particles are classified under the title ''cells and bioparticles'', and different kinds of nanoparticles are classified under the title of ''nanoparticles'' in the table).

Unique dielectric signature of the bioparticles has also been utilized for the detection and characterization. By measuring the cross-over frequencies, DEP can be utilized to follow the physiological state of the T-lymphocyte cells [149], to discriminate bovine red blood cells of different starvation ages [124, 150], and to detect and quantify hybridized DNA molecules on nano-genetic particles [151]. Srivasta et al. [152] was able to characterize red blood cells to identify blood type by examining the vertical and horizontal movement of the cells in a non-uniform electric field, and this was performed without any pretreatment or cell modification beyond simple blood dilution.

Liu and Garimella [142] proposed to utilize twDEP for actuating colloidal suspensions. They showed that by the interaction of the particle with the surrounding fluid, the particles that are put into motion by twDEP can generate fluid flow inside the microfluidic channel, and addressed that this proposed technique can be utilized for the pumping of nanofluids.

5 Concluding remarks

DEP is the movement of a particle in a non-uniform electric fields due to the interaction of the particle's dipole and spatial gradient of the electric field. It is subtle a solution to manipulate particles at microscale due to its favorable scaling effects. Depending on the dielectric properties of the particle and the medium, either positive or negative force can be generated. Unlike other affinity-based, fluorescence-based or magnetic-based manipulation methods, it does not require any labeling. DEP can be utilized either by DC-field or AC-field. In this work, a detailed analysis of the modeling of DEP-based manipulation of the particles is provided, and the recent applications regarding the particle manipulation in microfluidic systems are presented. Mainly, the published works between 2007 and 2010 have been focused on. Although many studies have been published, there are still some challenges that needs to be explored before DEP-based microfluidic devices meet end users. Regarding these challenges, possible future research directions on DEP research can be listed as follows:

(i) One of the ultimate goal of the microfluidics technology is to replace the bench-top instruments for clinical application. Regarding its advantages, DEP-based systems can be a perfect candidate to handle many tasks for the clinical applications. However, compared to the conventional techniques, throughput of the DEP-based systems are low, therefore throughput of the DEP-based systems need to be increased to make them competitive with the conventional instruments. Although some systems have been proposed for high throughput, more studies needs to be performed to improve the throughput of the DEP-based systems.

(ii) Another goal for the microfluidics technology is to develop hand-held, point-of-care testing devices. Although the microfluidic devices to handle DEP-based manipulation are simple, the instruments needed to run the system may be complex and bulky. Moreover, these devices or the preparation of the sample to run the system may need technical skills. Therefore, an integrated device with simple instrumentation that can handle both the sample preparation and the chemical/biological analysis is still a challenge for many applications.

(iii) Systems with internal electrodes offer many advantages. However, the fabrication of the internal electrodes are relatively expensive and complex compared to iDEP devices. Moreover, the fabrication procedures are not suitable for mass production. One alternative to this issue can be the use of the polymer-based conductive materials as electrodes and the fabrication of the microfluidic devices using mechanical micromachining (milling, drilling), microinjection molding techniques [153, 154]. Utilization of these techniques for the fabrication of the electrodes may lead to inexpensive and massive fabrication of DEP-based microfluidic systems.

(iv) For AC-DEP applications, DEP spectra of the cells and bioparticles is a very crucial parameter for the success of the analysis. Conventional method to obtain the DEP spectra is the electrorotation analysis. Electrorotation requires a special electrode design, and some specific equipments. Moreover, many data needs to be collected to come up with a statistically reliable data which makes it time-consuming. An alternative

method, to obtain these DEP spectra in a faster manner can be single-cell dielectric spectroscopy [120]. Integration of this new method with DEP-based systems would outcome robust and practical DEP-based clinical instruments.

(v) Although in many studies in the literature, particles are suspended in dilute buffer solutions, dealing with some bioparticles requires suspension of particles in a high-conductivity buffer solution. When the conductivity of the medium is much higher than the particle, it is impossible to generate positive forces with DEP. Therefore, the extension of the proposed systems that operate with high-conductivity buffer solutions can be a future research direction.

(vi) Manipulation of CNTs and nanoparticles are relatively new for DEP community, and patterning of CNTs and nanoparticles in precise manner is offering many emerging technologies. Therefore, optimum device designs for the precise control of the assemble of the CNTs and nanoparticles is still a rich research area for the near future of DEP research.

Financial support from the Middle East Technical University – Northern Cyprus Campus via the Campus Research Project (BAP-FEN10) is greatly appreciated.

The authors have declared no conflict of interest.

6 References

[1] Grier, D. G., *Nature* 2003, *424*, 810–816.

[2] McCloskey, K. E., Chalmers, J. J., Zborowski, M., *Anal. Chem.* 2003, *75*, 6868–6874.

[3] Nilsson, A., Petersson, F., Jonsson, H., Laurell, T., *Lab Chip* 2004, *4*, 131–135.

[4] Lapizco-Encinas, B.-H., Simmons, B. A., Cummings, E. B., Fintschenko, Y., *Electrophoresis* 2004, *25*, 1695–1704.

[5] Lapizco-Encinas, B.-H., Simmons, B. A., Cummings, E. B., Fintschenko, Y., *Anal. Chem.* 2004, *76*, 1571–1579.

[6] Kang, Y., Li, D., Kalams, S. A., Eid, J. E., *Biomed. Microdev.* 2008, *10*, 243–249.

[7] Barbulovic-Nad, I., Xuan, X., Lee, J. S. H., Li, D., *Lab Chip* 2006, *6*, 274–279.

[8] Kang, K. H., Xuan, X., Kang, Y., Li, D., *J. Appl. Phys.* 2006, *99*, 1–8.

[9] Kang, K. H., Kang, Y., Xuan, X., Li, D., *Electrophoresis* 2006, *27*, 694–702.

[10] Gallo-Villanueva, R.-C., Rodriguez-Lopez, C.-E., Diaz-de-la Garza, R.-I., Reyes-Betanzo, C., Lapizco-Encinas, B.-H., *Electrophoresis* 2009, *30*, 4195–4205.

[11] Moncada-Hernndez, H., Lapizco-Encinas, B.-H., *Anal. Bioanal. Chem.* 2010, *396*, 1805–1816.

[12] Zhu, J., Xuan, X., *Electrophoresis* 2009, *30*, 2668–2675.

[13] Chen, D., Du, H., Tay, C. Y., *Nanoscale Res. Lett.* 2010, *5*, 55–60.

[14] Zhu, J., Xuan, X., *J. Colloid Interf. Sci.* 2009, *3*, 2668–2675.

[15] Zhu, J., Tzeng, T.-R. J., Hu, G., Xuan, X., *Microfluid. Nanofluid.* 2009, *7*, 751–756.

[16] Zhu, J., Tzeng, T.-R. J., Xuan, X., *Electrophoresis* 2010, *31*, 1382–1388.

[17] Becker, F. F., Wang, X.-B., Huang, Y., Pethig, R., Vykoukal, J., *Proc. Natl. Acad. Sci. USA* 1995, *92*, 860–864.

[18] Gascoyne, P. R. C., Wang, X.-B., Huang, Y., Becker, F. F., *IEEE Trans. Ind. Appl.* 1997, *33*, 670–678.

[19] Rousselet, J., Markx, G. H., Pethig, R., *Colloid Surf. A* 1998, *140*, 209–216.

[20] Yang, J., Huang, Y., Wang, X.-B., Becker, F., Gascoyne, P., *Biophys. J.* 2000, *78*, 2680–2689.

[21] Gascoyne, P., Mahidol, C., Ruchirawat, M., Satayavivad, J., Watcharasit, P., Becker, F.-F., *Lab Chip* 2002, *2*, 70–75.

[22] Gascoyne, P. R. C., Satayavivad, J., Ruchirawat, M., *Acta Trop.* 2004, *89*, 357–369.

[23] Oblak, J., Krizaj, S. A. D., Macek-Lebar, A., Miklavcic, D., *Bioelectrochemistry* 2007, *71*, 164–171.

[24] Pommer, M. S., Zhang, Y., Keerthi, N., Chen, D., Thomson, J. A., Meinhart, C. D., Soh, H., *Electrophoresis* 2008, *29*, 1213–1218.

[25] Ji, H. M., Samper, V., Chen, Y., Heng, C., Lim, T. M., Yobas, L., *Biomed. Microdev.* 2008, *10*, 251–257.

[26] Markx, G. H., Pethig, R., *Biotechnol. Bioeng.* 1995, *45*, 337–343.

[27] Huang, J.-T., Wang, G.-C., Tseng, K.-M., Fang, S.-B., *J. Ind. Microb. Biotechnol.* 2008, *35*, 1551–1557.

[28] Vahey, M. D., Voldman, J., *Anal. Chem.* 2008, *80*, 3135–3143.

[29] Khoshmanesh, K., Zhang, C., Tovar-Lopez, F.-J., Nahavandi, S., Baratchi, S., Mitchell, A., Kalantar-Zadeh, K., *Microfluid. Nanofluid.* 2010, *9*, 411–426.

[30] Choi, W., Kim, J.-S., Lee, D.-H., Lee, K.-K., Koo, D.-B., Park, J.-K., *Biomed. Microdev.* 2008, *10*, 337–345.

[31] Flanagan, L. A., Lu, J., Wang, L., Marchenko, S. A., Jeon, N. L., Lee, A. P., *Stem Cells* 2008, *26*, 656–665.

[32] Borgatti, M., Bianchi, N., Mancini, I., Feriotto, G., Gambari, R., *Int. J. Mol. Med.* 2008, *21*, 3–12.

[33] Kim, U., Qian, J., Kenrick, S. A., Daugherty, P. S., Soh, H. T., *Anal. Chem.* 2008, *80*, 8656–8661.

[34] Sankaran, B., Racic, M., Tona, A., Rao, M. V., Gaitan, M., Forry, S. P., *Electrophoresis* 2008, *29*, 5047–5054.

[35] Du, J.-R., Juang, Y.-J., Wu, J.-T., Wei, H.-H., *Biomicrofluidics* 2008, *2*, 044103.

[36] Yin, Z., Noren, D., Wang, C. J., Hang, R., Levchenko, A., *Mol. Syst. Biol.* 2008, *4*, 232.

[37] de-la Rosa, C., Tilley, P., Fox, J. D., Kaler, K. V. I. S., *IEEE Trans. Biomed. Eng.* 2008, *55*, 2426–2432.

[38] Ravula, S. K., Branch, D. W., James, C. D., Townsend, R. T., Hill, M., Kaduchak, G., Ward, M., Brener, I., *Sensor Actaut. B* 2008, *130*, 645–652.

[39] Urdaneta, M., Smela, E., *Lab Chip* 2008, *8*, 550–556.

[40] Chu, H., Doh, I., Cho, Y.-H., *Lab Chip* 2009, *9*, 686–691.

[41] Moon, H.-S., Nam, Y.-W., Park, J. C., Jung, H.-I., *Environ. Sci. Technol.* 2009, *43*, 5857–5863.

[42] Thomas, R. S. W., Mitchell, P. D., Oreffo, R. O. C., Morgan, H., *Biomicrofluidics* 2010, *4*, 022806.

[43] Park, H., Kim, D., Yun, K.-S., *Sensor Actuat. B – Chem.* 2010, *150*, 167–173.

[44] Ghubade, A., Mandal, S., Chaudhury, R., Singh, R. K., Bhattacharya, S., *Biomed. Microdev.* 2009, *11*, 987–995.

[45] Kostner, S., van-der Driesche, S., Witarski, W., Pastorekova, S., Vellekoop, M. J., *IEEE Sensor J.* 2010, *10*, 1440–1446.

[46] Hirota, Y., Hakoda, M., Wakizaka, Y., *Bioprocess Biosyst. Eng.* 2010, *33*, 607–612.

[47] Yang, F., Yang, X., Jiang, H., Bulkhaults, P., Wood, P., Wang, W. H. G., *Biomicrofluidics* 2010, *4*, 013204.

[48] Chen, D., Du, H., *Microfluid. Nanofluid.* 2007, *3*, 603–610.

[49] Lewpiriyawong, N., Yang, C., Lam, Y. C., *Electrophoresis* 2010, *31*, 2622–2631.

[50] Khoshmanesh, K., Zhang, C., Tovar-Lopez, F.-J., Nahavandi, S., Baratchi, S., Kalantar-zadeh, K., Mitchell, A., *Electrophoresis* 2009, *30*, 3707–3717.

[51] Krishnan, J. N., Kim, C., Park, H. J., Kang, J. Y., Kim, T. S., Kim, S. K., *Electrophoresis* 2009, *30*, 1457–1463.

[52] Beech, J. P., Jonsson, P., Tegenfeldt, J. O., *Lab Chip* 2009, *9*, 2698–2706.

[53] Yu, C., Vykoukal, J., Vykoukal, D. M., Schwartz, J. A., Shi, L., Gascoyne, P., *J. Microelectromech. S.* 2005, *14*, 480–487.

[54] Yasukawa, T., Suzuki, M., Sekiya, T., Shiku, H., Matsue, T., *Biosens. Bioelectron.* 2007, *22*, 2730–2736.

[55] Cheng, I. F., Froude, V. E., Zhu, Y., Chang, H.-C., Chang, H.-C., *Lab Chip* 2009, *9*, 3193–3201.

[56] Lin, R.-Z., Ho, C.-H.-L. C.-T., Chang, H.-Y., *Biotechnol. J.* 2006, *1*, 949–957.

[57] Hsiung, L.-C., Yang, C. H., Chiu, C. L., Chen, C.-L., Wang, Y., Lee, H., Cheng, J.-Y., Ho, M.-C., Wo, A. M., *Biosens. Bioelectron.* 2008, *24*, 869–875.

[58] Suzuki, M., Yakusawa, T., Shiku, H., Matsue, T., *Biosens. Bioelectron.* 2008, *24*, 1043–1047.

[59] Park, K., Suk, H.-J., Akin, D., Bashir, R., *Lab Chip* 2009, *9*, 2224–2229.

[60] Tsutsui, H., Yu, E., Marquina, S., Valamehr, B., Wong, I., Wu, H., Ho, C.-M., *Ann. Biomed. Eng.* 2010, *38*, 3777–3788.

[61] Yu, L., Iliescu, C., Xu, G., Tay, F. E. H., *J. Microelectromech. S.* 2007, *16*, 1120–1129.

[62] Wang, L., Flanagan, L. A., Lee, A. P., *J. Microelectromech. S.* 2007, *16*, 454–461.

[63] Wang, L., Lu, J., Marchenko, S. A., Monuki, E., Flanagan, L. A., Lee, A. P., *Electrophoresis* 2009, *30*, 782–791.

[64] Kang, Y., Cetin, B., Wu, Z., Li, D., *Electrochim. Acta* 2009, *54*, 1715–1720.

[65] Cetin, B., Kang, Y., Wu, Z., Li, D., *Electrophoresis* 2009, *30*, 766–772.

[66] Cetin, B., Li, D., *Electrophoresis* 2009, *30*, 3124–33133.

[67] Cetin, B., Li, D., *Electrophoresis* 2010, *31*, 3035–3043.

[68] Demierre, N., Braschler, T., Linderholm, P., Seger, U., van Lintel, H., Renaud, P., *Lab Chip* 2007, *7*, 355–365.

[69] Valero, A., Braschler, T., Demierre, N., Renaud, P., *Biomicrofluidics* 2010, *4*, 022807.

[70] Mernier, G., Piacentini, N., Braschler, T., Demierre, N., Renaud, P., *Lab Chip* 2010, *10*, 2077–2082.

[71] Martinez-Duarte, R., Gorkin, R. A., III, Abi-SamatralII, K., Madou, M. J., *Lab Chip* 2010, *10*, 1030–1043.

[72] Jaramillo, M.-d.-C., Torrents, E., Martinez-Duarte, R., Madou, M., Juarez, A., *Electrophoresis* 2010, *31*, 2921–2928.

[73] Shafiee, H., Sano, M. B., Henslee, E. A., Caldwell, J. L., Davalos, R. V., *Lab Chip* 2010, *10*, 438–445.

[74] Choi, E., Kim, B., Park, J., *J. Micromech. Microeng.* 2009, *19*, 125014.

[75] Khoshmanesh, K., Zhang, C., Nahavandi, S., Baratchi, S., Michael, A., Kalantar-zadeh, K., *Electrophoresis* 2010, *31*, 3380–3390.

[76] Hughes, M. P., Morgan, H., Rixon, F. J., Burt, J. P. H., Pethig, R., *Biochim. Biophys. Acta* 1998, *1425*, 119–126.

[77] Hubner, Y., Hoettges, K. F., McDonnell, M. C., Carter, M. J., Hughes, M. P., *Int. J. Nanomed.* 2007, *2*, 427–431.

[78] Cummings, E. B., Singh, A. K., *Anal. Chem.* 2007, *75*, 4724–4731.

[79] Khoshmanesh, K., Zhang, C., Campbell, J. L., Kayani, A. A., Nahavandi, S., Baratchi, S., Kalantar-zadeh, A.-M. I. K., *Microfluid. Nanofluid.* 2010, *9*, 755–763.

[80] Krishnan, R., Sullivan, B. D., Mifflin, R. L., Esener, S. C., Heller, M. J., *Electrophoresis* 2008, *29*, 1765–1774.

[81] Shin, D. H., Kim, J.-E., Shim, H. C., Song, J.-W., Yoon, J.-H., Kim, J., Jeong, S., Kang, J., Baik, S., Han, C.-S., *Nano Lett.* 2008, *8*, 4380–4385.

[82] Padmaraj, D., Zagozdzon-Wosik, W., Xie, L. M., Hadjiev, V. G., Cherukuri, P., Wosik, J., *Nanotechnology* 2009, *20*, 035201.

[83] Wei, C., Wei, T.-Y., Tai, F.-C., *Diam. Relat. Mater.* 2010, *8*, 609–617.

[84] Zhang, C., Khoshmanesh, K., Tovar-Lopez, F. J., Mitchell, A., Wlodarski, W., Klantar-zadeh, K., *Microfluid. Nanofluid.* 2009, *7*, 633–645.

[85] Suehiro, J., *Biomicrofluidics* 2010, *4*, 022804.

[86] Xu, D., Subramanian, A., Dong, L., Nelson, B. J., *IEEE Trans. Nanotechnol.* 2009, *8*, 449–456.

[87] Xu, D., Shou, K., Nelson, B. J., *Microelectron. Eng.* 2011, *88*, 2703–2706.

[88] Ferrara, V. L., Alfano, B., Massera, E., Francia, G. D., *IEEE Trans. Nanotechnol.* 2008, *7*, 776–781.

[89] Lee, M.-W., Lin, Y.-H., Lee, G.-B., *Microfluid. Nanofluid.* 2010, *8*, 609–617.

[90] Castillo, J., Tanzi, S., Dimaki, M., Svendsen, W., *Electrophoresis* 2008, *29*, 5026–5032.

[91] Hawkins, B. G., Smith, A. E., Syed, Y. A., Kirby, B. J., *Anal. Chem.* 2007, *79*, 7291–7300.

[92] Lewpiriyawong, N., Yang, C., Lam, Y. C., *Biomicrofluidics* 2008, *2*, 034105-1–034105-7.

[93] Church, C., Zhu, J., Nieto, J., Keten, G., Ibarra, E., Xuan, X., *J. Micromech. Microeng.* 2010, *20*, 065011.

[94] Prinz, C., Tegenfeldt, J., Austin, R., Cox, E., Sturm, J., *Lab Chip* 2002, *2*, 207–212.

[95] Chou, C.-F., Zenhausern, F., *IEEE Eng. Med. Biol.* 2003, *22*, 62–67.

[96] Church, C., Zhu, J., Wang, G., Tzeng, T.-R. J., Xuan, X., *Biomicrofluidics* 2009, *340*, 044109.

[97] Regtmeier, J., Eichhorn, R., Bogunovic, L., Ros, A., Anselmetti, D., *Anal. Chem.* 2010, *82*, 7141–7149.

[98] Baylon-Cardiel, J.-L., Jesus-Perez, N.-M., Chavez-Santoscoya, A.-V., Lapizco-Encinas, B.-H., *Lab Chip* 2010, *10*, 3235–3242.

[99] Jen, C.-P., Huang, C.-T., Weng, C.-H., *Microelectron. Eng.* 2010, *87*, 773–777.

[100] Voldman, J., *Annu. Rev. Biomed. Eng.* 2006, *8*, 425–454.

[101] Cetin, B., Li, D., *Electrophoresis* 2008, *29*, 994–1005.

[102] Morgan, H., Green, N. G., *AC Electrokinetics: Colloids and Nanoparticles*, Research Studies Press, London 2003, pp. 8–12.

[103] Markx, G. H., Davey, C. L., *Enzyme Microb. Technol.* 1999, *25*, 161–171.

[104] Jones, T. B., *Electromechanics of Particles*, Cambridge University Press, Cambridge 1995, pp. 34–48, 110–138.

[105] Gascoyne, P. R. C., Vykoukal, J., *Electrophoresis* 2002, *23*, 1973–1983.

[106] Jones, T. B., Washizu, M., *J. Electrostat.* 1996, *37*, 121–134.

[107] Wang, X., Wang, X.-B., Gascoyne, P. R. C., *J. Electrostat.* 1997, *39*, 277–295.

[108] Pethig, R., *Biomicrofluidics* 2010, *4*, 022811.

[109] Al-Jarro, A., Paul, J., Thomas, D. W. P., Crowe, J., Sawyer, N., Rose, F. R. A., Shakesheff, K. M., *J. Phys. D: Appl. Phys.* 2007, *40*, 71–77.

[110] Park, S., Beskok, A., *Anal. Chem.* 2008, *80*, 2832–2841.

[111] Castellanos, A., Ramos, A., Gonzalez, A., Green, N. G., Morgan, H., *J. Phys. D: Appl. Phys.* 2003, *36*, 2584–2597.

[112] Cetin, B., PhD Thesis, Vanderbilt University, Nashville, TN, USA 2009.

[113] Green, N. G., Morgan, H., *J. Phys. Chem. B* 1999, *103*, 41–50.

[114] Eppmann, P., Gimsa, B. P. J., *Colloid Surf. A* 1999, *149*, 443–449.

[115] Ermolina, I., Morgan, H., *J. Colloid Interf. Sci.* 2005, *285*, 419–428.

[116] Yih, T. C., Talpasanu, I., *Micro and Nano Manipulations for Biomedical Applications*, Artech House , Boston, USA 2008, pp. 191–202.

[117] Turcu, I., Lucaciu, C. M., *J. Phys. A: Math. Gen.* 1989, *22*, 985–993.

[118] Gascoyne, P. R. C., Vykoukal, J., *Proc. IEEE* 2004, *92*, 22–42.

[119] Polevaya, Y., Ermolina, I., Schlesinger, M., Ginzburg, B.-Z., Feldman, Y., *Biochim. Biophys. Acta* 1999, *1419*, 257–271.

[120] Valero, A., Braschler, T., Renaud, P., *Lab Chip* 2010, *10*, 2216–2225.

[121] Wang, X., Huang, Y., Gascoyne, P. R. C., Becker, F. F., Holzel, R., Pethig, R., *Biochim. Biophys. Acta* 1994, *1193*, 330–344.

[122] Chan, K. L., Gascoyne, P. R. C., Becker, F. F., Pethig, R., *Biochim. Biophys. Acta* 1997, *1349*, 182–196.

[123] Dalton, C., Goater, A. D., Drysdale, J., Pethig, R., *Colloid Surf. A* 2001, *195*, 263–268.

[124] Gagnon, Z., Gordon, J., Sengupta, S., Chang, H.-C., *Electrophoresis* 2008, *29*, 2272–2279.

[125] Cruz, J. M., Garcia-Diego, F. J., *J. Phys. D: Appl. Phys.* 1998, *31*, 1745–1751.

[126] Green, N. G., Jones, T. B., *J. Phys. D: Appl. Phys.* 2007, *40*, 78–85.

[127] Sanchis, A., Brown, A. P., Sancho, M., Martinez, G., Sebastian, J. L., Munoz, S., Miranda, J. M., *Bioelectromagnetics* 2007, *28*, 393–401.

[128] Winter, W. T., Welland, M. E., *J. Phys. D: Appl. Phys.* 2009, *42*, 045501.

[129] Green, N., Ramos, A., Gonzalez, A., Morgan, H., Castellanos, A., *Phys. Rev. E* 2002, *66*, 026305.

[130] Cetin, B., Li, D., *ASME IMECE 08*, Boston, MA, USA 2008.

[131] Chen, K. P., Pacheco, J. R., Hayes, M. A., Staton, S. J. R., *Electrophoresis* 2009, *30*, 1441–1448.

[132] Ai, Y., Joo, S. W., Jiang, Y., Xuan, X., Qian, S., *Electrophoresis* 2009, *30*, 2499–2506.

[133] Ai, Y., Joo, S. W., Jiang, Y., Xuan, X., Qian, S., *Biomicrofluidics* 2009, *3*, 022404.

[134] Ai, Y., Qian, S., *J. Colloid Interf. Sci.* 2010, *346*, 448–454.

[135] Ai, Y., Park, S., Zhu, J., Xuan, X., Beskok, A., Qian, S., *Langmuir* 2010, *26*, 2937–2944.

[136] Ai, Y., Beskok, A., Gauthier, D. T., Joo, S. W., Qian, S., *Biomicrofluidics* 2009, *3*, 044110.

[137] Leal, L. G., *Advanced Transport Phenomena: Fluid Mechanics and Convective Transport Processes*, Artech House, New York, USA 2006, pp. 164–168.

[138] Berthier, J., Silberzan, P., *Microfluidics for Biotechnology*, Cambridge University Press, Cambridge, USA 2007, pp. 320–325.

[139] Benselama, A. M., Pham, P., Canot, E., *Technical Proceedings of the 2004 NSTI Nanotechnology Conference and Trade Show*, Cambridge, USA vol. 1, 2004.

[140] Park, J. S., Saintillan, D., *J. Fluid. Mech.* 2010, *662*, 66–90.

[141] Park, J. S., Saintillan, D., *Phys. Rev. E* 2011, *83*, 041409.

[142] Liu, D., Garimella, S. V., *Nanosc. Microsc. Therm.* 2009, *13*, 109–133.

[143] Cummings, E., Khusid, B., in: Hardt, S., Schönfeld, F. (Eds.), *Microfluidic Technologies for Miniaturized Analysis Systems*. Springer, USA 2007, pp. 315–351.

[144] Pethig, R., Markx, G. H., *Trends Biotechnol.* 1997, *15*, 426–432.

[145] Pethig, R., Burt, J. P. H., Parton, A., Rizvi, N., Talary, M. S., Tame, J. A., *J. Micromech. Microeng.* 1998, *8*, 57–63.

[146] Burgarella, S., Merlo, S., Dell'Anna, B., Zarola, G., Bianchessi, M., *Microelectron. Eng.* 2010, *87*, 2124–2133.

[147] Iliescu, C., Yu, G. L., Samper, V., Tay, F. E. H., *J. Micromech. Microeng.* 2005, *15*, 494–500.

[148] Wang, L., Flanagan, L. A., Jeon, N. L., Monuki, E., Lee, A. P., *Lab Chip* 2007, *7*, 1114–1120.

[149] Pethig, R., Bressier, V., Carswell-Crumpton, C., Chen, Y., Foster-Haje, L., Garcia-Ojeda, M.-E., Lee, R. S., Lock, G. M., Talary, M. S., Tate, K. M., *Electrophoresis* 2002, *23*, 2057–2063.

[150] Gordon, J. E., Gagnon, Z., Changa, H.-C., *Biomicrofluidics* 2007, *1*, 044102.

[151] Gagnon, Z., Senapati, S., Gordon, J., Chang, H.-C., *Electrophoresis* 2008, *29*, 4808–4812.

[152] Srivastava, S. K., Daggolu, P. R., Burgess, S. C., Minerick, A. R., *Electrophoresis* 2008, *29*, 5033–5046.

[153] Jung, W.-C., Heo, Y.-M., Yoon, G.-S., Shin, K.-H., Chang, S.-H., Kim, G.-H., Cho, M.-W., *Sensors* 2007, *7*, 1643–1654.

[154] Griffiths, C. A., Dimova, S., Hirshy, H., Scholza, S., Fischerb, S., Spitzbart, M., *ICOMM 2011*, March 7–10, Tokyo, Japan 2011.

